Effect of rock density on the response of scour protection to earthquake-induced liquefaction for offshore wind applications

Diarmid M Xu, Gopal Madabhushi, C N Abadie, John M Harris, Richard J S Whitehouse

Effect of rock density on the response of scour protection to earthquake-induced liquefaction for offshore wind applications

D.M. Xu, S.P.G. Madabhushi & C.N. Abadie
Department of Engineering, University of Cambridge, Cambridge, UK

J.M. Harris & R.J.S. Whitehouse
HR Wallingford, Wallingford, UK

ABSTRACT: Offshore wind is an expanding source of renewable energy, with new wind farms currently developed in seismically active zones. The presence of loose, liquefiable sands raises concerns regarding the behaviour of the scour protection rock for foundation of offshore structures during an earthquake, namely the large settlement of the rock berm (Xu et al., 2022), but there is little understanding of best practice in the design. This paper presents the results of two dynamic centrifuge tests that explore the effect of rock density on berm settlement due to earthquake induced liquefaction of the seabed. The collected data capture rock settlement, soil accelerations and pore pressures within the models. The results show that significant settlements occur for all scour protection rock types, but higher density rock is susceptible to larger settlements. The results form part of a wider project researching the behaviour of rock scour protection in liquefiable soils.

1 Introduction

Offshore wind is an ever-growing industry with huge potential to meet the future demand of renewable energy (Global Energy Review 2021, 2021). As global energy usage increases, new offshore wind farm developments are being constructed in seismically active areas, such as North America and East Asia. The most common type of foundation selected for offshore wind turbines is the monopile, large diameter steel tubes that are hammered into the seabed (Deep Water, 2013).

In scour prone areas, rock dump is used to lay a rock berm around the monopile, either as a preventative measure or as remediation. Scour is a phenomenon where the water currents that collide with the foundation are redirected into vortices that erode away the sediment around the foundation (Harris et al., 2019).

A typical berm geometry for an example 8m diameter pile would have a filter and armour rock layer spanning five and three times the monopile diameter respectively (The Rock Manual, 2007). Armour rock are typically larger, at 0.3m to 0.5m in diameter, they resist the push of the current whereas the filter rocks are smaller, 0.1m to 0.2m and they prevent the armour rocks from sinking into the sand. Each layer is around 0.5m to 1.0m thick. An alternative approach to the lays above is 1-2m of well graded rock (widely graded on a Particle Size Distribution plot) rock dump that can serve both functions. The exact rocks used varies per site so the dimensions and berm thicknesses given here are only representative values.

Both the monopile and rock dump are a common and cost-effective way of building turbine foundations, however, while the phenomenon of scour is relatively well documented and studied (Harris and Whitehouse, 2017) (Harris et al., 2019) (Whitehouse and Draper, 2020), there is little data or research into the seismic behaviour of rock scour protection, specifically settlement induced by liquefaction (Escribano and Brennan 2017).

Recent research has studied the effectiveness of different types of protection and their effect on restoring foundation stiffness and strength (Mayall et al., 2020), however, design codes provide limited or conservative methods (Standard DNV GL, 2016, Standard DNV GL 2021). Three options are given to design against scour for offshore monopiles:

- install scour protection before or shortly after foundation installation, or;
- specify a pile embedment length that remains sufficiently long even after the most extreme case of scour, or;
- "monitor and react", with appropriate pile embedment length designed with a scour allowance, and scour remediation work is only carried out if and when required.

It is also stated that scour must be considered during design but there is limited guidance on how this should be done. The three options are all costly, either due to over design of the foundation, or scour

protection, or through the risk of future remediation. Therefore, understanding seismic impact is important.

Both Escribano and Brennan (2017) and Xu et al. (2022) showed significant settlement of the scour protection rocks, of around 0.35m. In this paper, the results of two saturated dynamic centrifuge tests that continue the research of Xu et al. (2022) are presented, with focus on the effect of rock density on rock settlement due to seismic liquefaction. Centrifuge tests named DMX02 and DMX03 differ only in the density of rock used, with DMX02 being the benchmark test using a mid-range rock specific gravity compared to a higher rock density in DMX03. In both tests, the rock and sand settlement, soil accelerations and pore water pressures were captured and compared.

2 Experimental Methodology

2.1 *Centrifuge testing*

A geotechnical centrifuge allows small scale models to be tested at elevated *g* levels, where the results, after scaling (Schofield, 1980), can be converted to match that of prototype structures out in the field. Centrifuge testing mitigates the need to carry out scale testing on prohibitively large civil engineering structures, while still allow the study of the non-linear behavior of soils.

The centrifuge used in this study was the 10 m-diameter Turner beam centrifuge at the Schofield Centre (Madabhushi, 2014). Two saturated dynamic centrifuge tests were performed at 50g in a model container sized 730mm x 250mm x 400mm and a servo hydraulic shaker was used to simulate a series of earthquakes (Madabhushi et al., 2012).

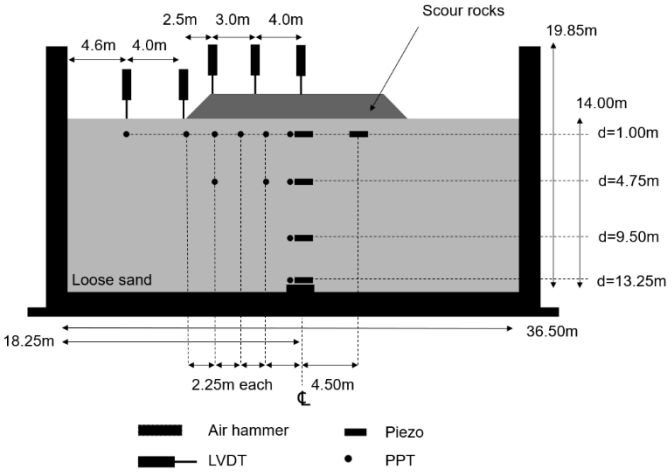

Figure 1. Test schematic of DMX03, prototype scale

Figure 1 shows a cross section of the model for DMX03. The sand and rock formation remained identical in DMX02 and DMX03, with only the rock density, but not the size or number of rocks used, being changed. Another slight variation was in the position of the sensors below the rock berm, in DMX03 more sensors were deployed, as shown in Figure 1. The sand was saturated with methylcellulose for scaling purposes. Figure 2 presents the berm geometry where D_{50} is the rock diameter. Sufficient space was given for the sand to flow and heave (so that the rock may settle) and to avoid boundary conditions.

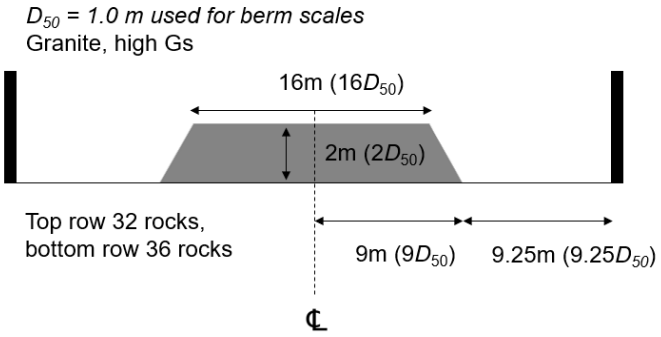

Figure 2. Berm geometry of DMX03, prototype scale

2.2 *Rock berm design*

The model rock berm represented a simplified worst case scenario, of two layers of poorly graded large 1m armour rocks with no filter layer. Due to the size of the rocks (20mm) and the size of the container, a checker board grid of rocks were laid to form the rock berm. This procedure was repeated for both tests, meaning the size and number of rocks used was identical.

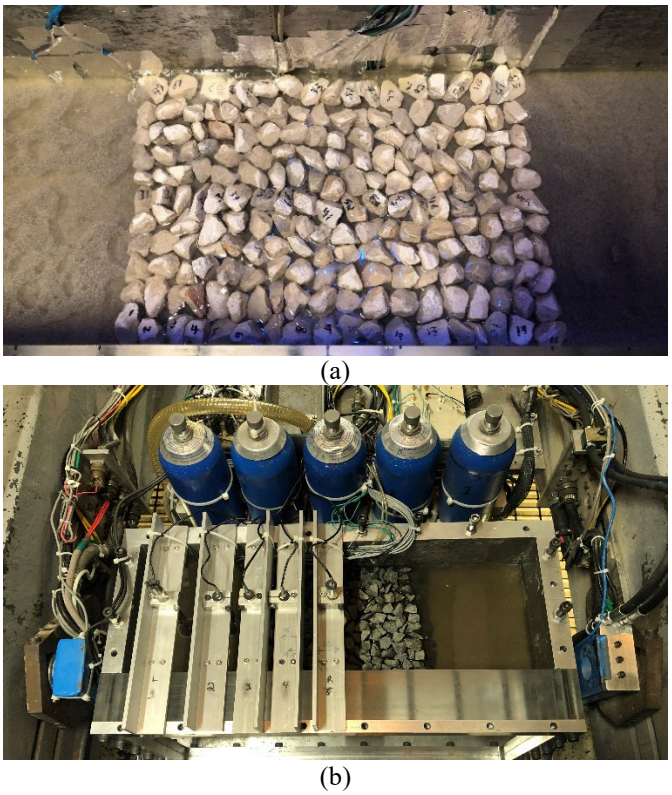

(a)

(b)

Figure 3(a). Top down view of model DMX02 and (b) DMX03, part of the view is blocked by gantries that hold LVDT sensors. The blue cylinders are part of the servo-hydraulic shaker.

DMX02 was the benchmark test, with a rock specific gravity of G_s=2.62. The heavier rocks of DMX03 had a G_s=2.88. Figure 3 shows the test models of both experiments. Note that the colours of the rocks are different but this has no effect on the results.

Table 1 is adapted from Xu et al. (2022) and summarises the model rock dimensions and properties. If the ratio D_{50}/d_{50}, that of the rock and sand in the field, was kept the same in the model, the size of the sand grains would more closely resemble that of clay, and thus the sediment behaviour would be incorrect. Madabhushi (2014) states that as long D_{50}/d_{50} is greater than 15, reasonable scaling of the rock and sand particles would be ensured.

Table 1. Comparison of berm rock properties *

Parameter	DMX02 (prototype)	DMX03 (prototype)	(Escribano and Brennan, 2017)	Field data
d_{50} (mm)	0.44	0.44	0.14	0.15
D_{50} (mm)	1000	1000	500	500-1000
t_s (mm)	2000	2000	1500	1500
t_s/D_{50}	2	2	3	3-1.5
D_{50}/d_{50}	2273	2273	3571	3333-6667
G_s	2.62	2.88	-	2.5-3.0

* (D_{50} is used for scour rock grading, and d_{50} used for sediment grading. t_s is the berm thickness/height.)

2.3 *Model soil*

The sand used was Hostun HN31, d_{50}=0.44mm, a sand that is manufactured, not quarried. This means the physical properties of the sand can be tightly controlled and measured (void ratio e_{min}=0.555, e_{max}=1.01, specific gravity G_s=2.65). While not a suitable sand for construction, it is a reliable, medium grained sand for scientific research.

The sand was poured to be loose, at a relative density of 43% using an automatic sand pourer as described in Madabhushi et al. (2006), to maintain uniformity and repeatability. After pouring, the sand was saturated with methylcellulose to ensure the correct liquid scaling. Saturation was achieved via controlled vacuum suction through a modified saturation system based on the system developed by Stringer and Madabhushi (2009).

2.4 *Load sequence*

A series of four earthquakes were fired using the servo-hydraulic shaker (Madabhushi et al., 2012), these are shown in Table 2. To begin, a small test earthquake (input Peak Ground Acceleration, i.e. bedrock acceleration, PGA~0.05g) is fired to ensure all systems and sensors are functioning correctly, this does not fully liquify the soil and little settlements occur. Next, two large earthquakes are fired (PGA~0.3g to 0.4g). Finally, to show that "soil remembers" its past loading history, a small earthquake (PGA~0.05g) is simulated to end the experiment, where little to no liquefaction or settlement is expected.

Table 2. Earthquake sequence for both DMX02 and DMX03

Earthquake number	Earthquake
EQ1	Kobe, 0.15V
EQ2	Sine wave, 50Hz, 15 cycles, 2.50V
EQ3	Sine wave, 50Hz, 15 cycles, 3.00V
EQ4	Sine wave, 50Hz, 15 cycles, 0.75V

2.5 *Instrumentation*

Sensors were installed during the sand pouring process at regular depth intervals. Linear variable displacement transducers (LVDT's) at the top track rock settlement and sand heave, zero displacement is defined to be at the starting position of each earthquake. Pore water pressure transducers (PPT's) and piezoelectric accelerometers capture pore water pressure and soil accelerations.

DASYLab v13.0 was used to log data into text files for processing later. A logging rate of 6000Hz was used for dynamic events, and a rate of 100Hz was used for swing up, to record pore pressures and settlements as the g level increases from one to fifty. Though that data is normally not used, if something were to go awry during the flight, these data could help identify the problem and when it occurred.

3 **Test Results**

All sensor voltages were first filtered, then calibrated and zeroed in MATLAB using a bespoke script, before being scaled to prototype scale. All results are presented at prototype scale. An eighth order Butterworth filter was used to reduce phase shift. An approximate initial effective vertical stress has been calculated to identify the limit of liquefaction, where r_u=1 (the ratio of excess pore pressure and initial effective vertical stress).

3.1 *Rock settlement*

Figure 4 shows some exemplar data from DMX03, EQ2 (PGA=0.4g), of the rock settlements versus the input motion at the bottom in blue. It is seen that significant rock settlement occurs, in the region of 0.75m with the middle of the berm settling more than the sides, this is corroborated by Figure 5, a post test image of the model where the berm can be seen to have curved. It is also observed that the sand heaves due to the rock settlement. Lastly, the settlement history shows a characteristic start stop motion that matches that of the input motion.

The settlements at the berm centre for all earthquakes are summarized in Figure 6, where the settlement has been plotted against the Arias Intensity, a measure of the energy of an earthquake. The Arias

Intensity is a value to compare earthquakes, for example, between a high amplitude, low cycle count quake and a low amplitude, high cycle one. From this data, it is seen that the grouping of higher settlement data points is reversed between the earthquakes for low and high Arias Intensities, i.e. in the case of low Arias Intensity, DMX02 resulted in higher settlements, whereas for high Arias Intensity, DMX03 was higher. This means that higher density rock settles more than mid-range density rock under full liquefaction (EQ2 and EQ3), but under partial liquefaction from smaller earthquakes, the settlement is less (EQ1 and EQ4). Figure 7 compares the time histories of EQ2 from both DMX02 and DMX03, the input motion is shown to be very similar, but the settlement from DMX03 is higher. In DMX03, 15 cycles of the sine wave was fired, instead of 10, but the comparative settlements shown in Figure 6 were taken at 10 cycles for both tests.

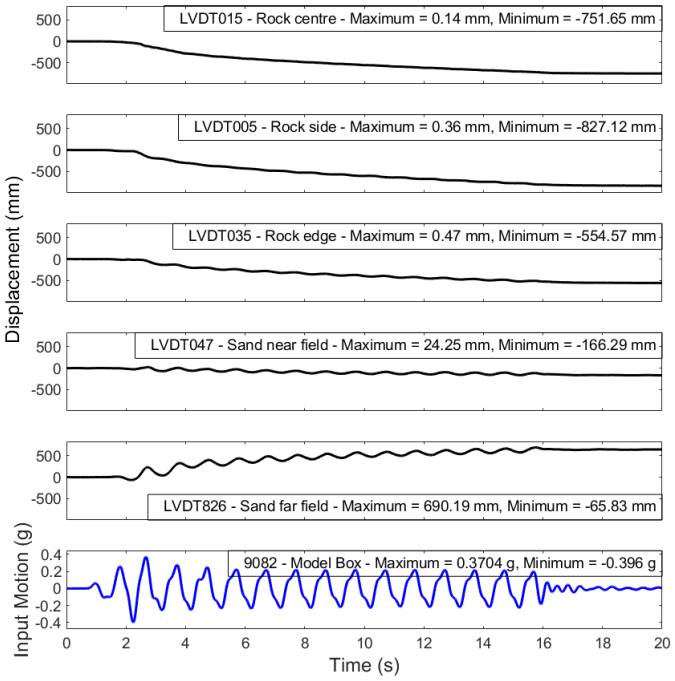

Figure 4. Displacement time history from EQ2 of DMX03 for all LVDT's including the input motion

As shown in Escribano and Brennan (2017) and Xu et al. (2022), the addition of a rock berm will increase the initial effective vertical stress, and thus delay the onset of full liquefaction. This delay will reduce rock settlement for smaller earthquakes, where full liquefaction does not occur. However, for larger input motions, full liquefaction does occur, at which point the higher density rocks will in fact settle more than their lighter counterparts.

3.2 *Soil liquefaction*

From the plot of excess pore water pressure in Figure 8, it is shown that the soil reaches full liquefaction under the larger earthquakes of EQ2 and EQ3. The selected sensors form the central column in Figure 1. The liquefaction limit line is an estimation, taking into account the weight of sand and that of the rock berm prior to the earthquake.

Figure 5. Post DMX03 image of the rock berm, side view

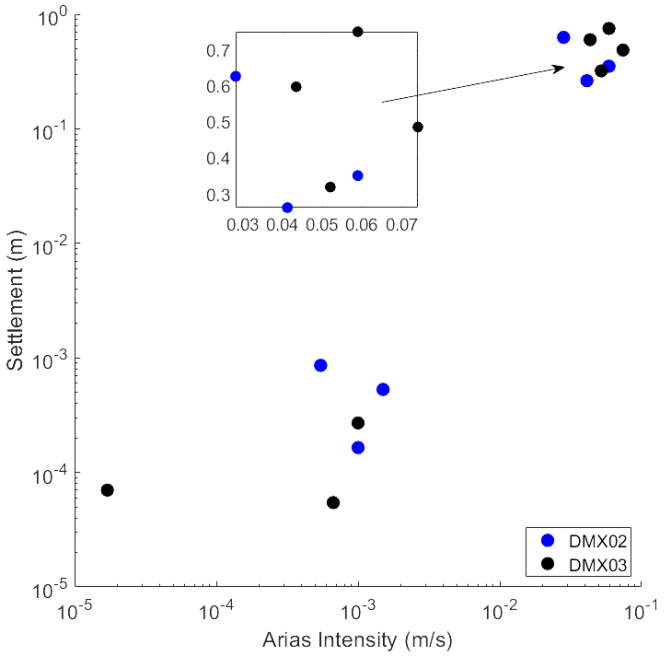

Figure 6. Summary of mid-berm settlements for all earthquakes from DMX02 and DMX03, separated by Arias Intensity, using logarithmic scales

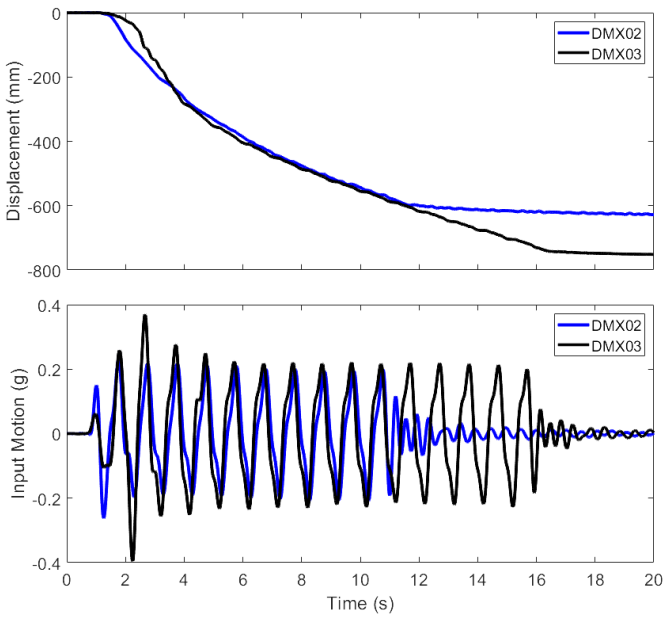

Figure 7. Comparison of EQ2 from DMX02 and DMX03

Full liquefaction is also confirmed in Figure 9 where decoupling can be seen in the (piezo recorded)

acceleration time history. As the shallow regions of sand liquefy, they can no longer transfer shear waves, and thus the acceleration time trace "fades" as the input motion travels up the soil column.

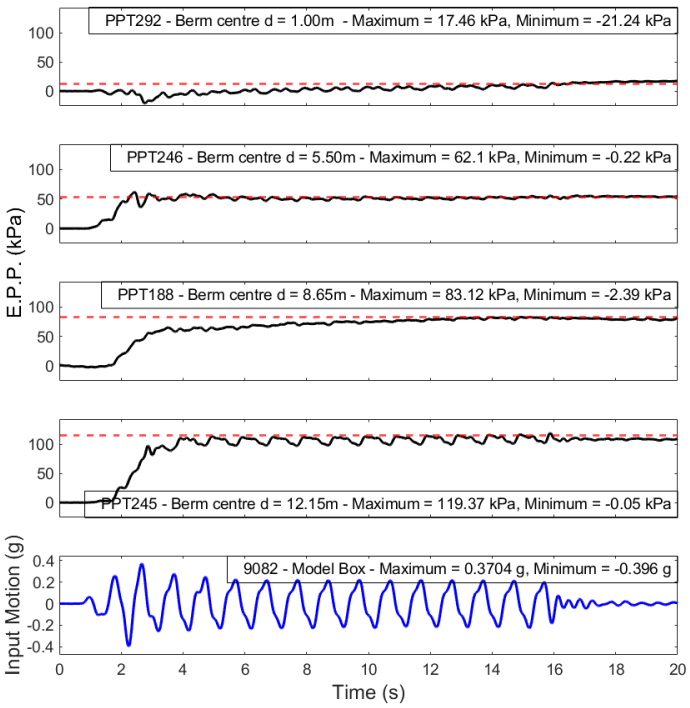

Figure 8. Excess pore pressure of EQ2, DMX03, central PPT stack, including liquefaction limit line (red) and input motion (blue)

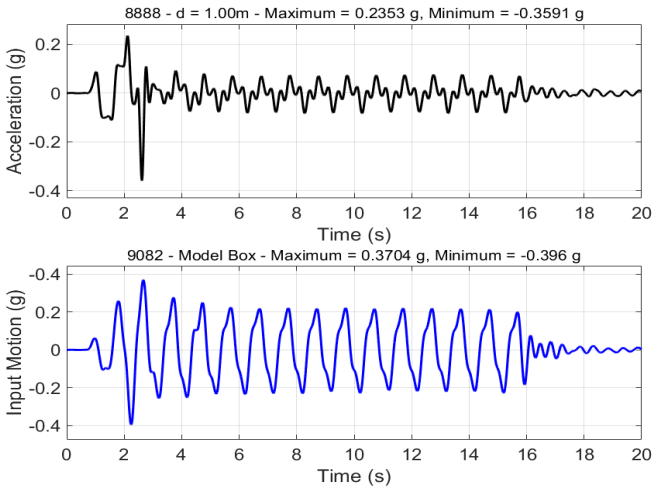

Figure 9. Selected acceleration time history plot from EQ2, DMX03, showing decoupling 1m below sand surface due to liquefaction

4 Conclusions

From the two centrifuge tests it can be seen that significant settlements can occur with any scour protection armour rock, however, under full liquefaction due to large earthquakes, the settlement of higher density rock will be greater compared to that of lower density rock.

Usually the rock to be used on a project is selected based on proximity to quarries, as a large proportion of the cost of rock dump is the transportation from the source to site. One reason high density rocks such as granite might be chosen, despite the higher unit cost than standard density rock, is to reduce the rock berm thickness required to ensure enough rock weight to resist scour currents and to add stiffness to the monopile foundation.

As seen from the results presented here, there is no major incentive to use high density rock dump to reduce scour protection rock settlement due to seismically induced liquefaction. For earthquakes producing high Arias Intensities, high density rock fill resulted in a 30% increase in the average and maximum recorded rock settlement in this study. However, a reduction of 75% settlement for quakes of low Arias Intensity was observed owing to the larger initial vertical effective stress imposed by the denser rocks.

Future planned work includes investigating the effect of rock size, rock grading and berm geometry on rock settlement post-earthquake. A monopile may also be included into future models. This research should form the basis for further research in the behaviour of rock scour protection in liquefiable soils.

5 Acknowledgements

The authors acknowledge the generous funding from EPSRC and HR Wallingford that made this project possible, and the help and advice of the technicians at the Schofield Centre.

REFERENCES

Deep Water (2013). Available at: http://www.ewea.org/fileadmin/files/library/publications/reports/Deep_Water.pdf.

Escribano, D. and Brennan, A. (2017). Stability of scour protection due to earthquake-induced liquefaction: Centrifuge modelling. Coastal Engineering, 129, pp. 50–58.

Global Energy Review 2021 (2021). Paris. Available at: https://www.iea.org/reports/global-energy-review-2021.

Harris, J. M. and Whitehouse, R. (2017) 'Scour Development around Large-Diameter Monopiles in Cohesive Soils: Evidence from the Field', Journal of Waterway, Port, Coastal, and Ocean Engineering, 143(5), p. 4017022. doi: 10.1061/(ASCE)WW.1943-5460.0000414.

Harris, J. M., Whitehouse, R.J.S., Tavouktsoglou, N.S., and Godinho, P.M. (2019) 'Foundation Scour as a Geohazard', Journal of Waterway, Port, Coastal, and Ocean Engineering, 145(6), p. 4019022. doi: 10.1061/(ASCE)WW.1943-5460.0000523.

Madabhushi, S.P.G., Houghton, N.E., Haigh, S.K. (2006). A new automatic sand pourer for model preparation at University of Cambridge, in: Physical Modelling in Geotechnics, 6th ICPMG'06 - Proceedings of the 6th International Conference on Physical Modelling in Geotechnics. pp. 217–222.

Madabhushi, G.S.P., Haigh, S.K., Houghton, N.E., and Gould, E. (2012). Development of a servo-hydraulic earthquake actuator for the Cambridge Turner beam centrifuge. International Journal of Physical Modelling in Geotechnics, 12(2), pp. 77–88.

Madabhushi, G.S.P. (2014). *Centrifuge Modelling for Civil Engineers*, *Centrifuge Modelling for Civil Engineers*. doi: 10.1201/9781315272863.

Mayall, R., McAdam, R.A., Whitehouse, R.J.S., Burd, H.J., Byrne, B.W., Heald, S.G., Sheil, B.B., and Slater, P.L. (2020). Flume tank testing of offshore wind turbine dynamics with foundation scour and scour protection. Journal of Waterway, Port, Coastal, and Ocean Engineering, 146(5), p. 4020033.

Schofield, A.N. (1980). Cambridge Geotechnical Centrifuge Operations. Géotechnique, 30(3), pp. 227–268.

Standard DNVGL-ST-0126. (2016). Available at: https://rules.dnv.com/docs/pdf/DNV/ST/2016-04/DNVGL-ST-0126.pdf.

Standard DNVGL-RP-0585. (2021). Available at: https://www.dnv.com/energy/standards-guidelines/dnv-rp-0585-seismic-design-of-wind-power-plants.html.

Stringer, M.E. and Madabhushi, S.P.G. (2009). Novel Computer-Controlled Saturation of Dynamic Centrifuge Models Using High Viscosity Fluids. Geotechnical Testing Journal - GEOTECH TESTING J, 32.

The Rock Manual. 2nd Edition (2007). Ciria.

Whitehouse, R. and Draper, S. (2020) 'Sediment transport and scour in the ocean environment - knowledge and future directions', in ISFOG. Available at: http://www.dfi.org/pubdetail.asp?id=3434.

Xu, D.M., Abadie, C.N., Madabhushi, G.S.P., Harris, J. M., and Whitehouse, R.J.S. (2022). Response of armour rock-scour protection to earthquake-induced liquefaction for offshore wind applications. 10th ICPMG 2022 - Proceedings of the 10th International Conference on Physical Modelling in Geotechnics. pp. 500-503.